

Sequential Growth of Magic-Size CdSe Nanocrystals**

By Stefan Kudera, Marco Zanella, Cinzia Giannini, Aurora Rizzo, Yanqin Li, Giuseppe Gigli, Roberto Cingolani, Giuseppe Ciccarella, Werner Spahl, Wolfgang J. Parak, and Liberato Manna*

Colloidal semiconductor nanocrystals have been exploited in several applications in which they serve as fluorophores, because of the tunability of the wavelength of the emitted light.^[1–3] The possibility of exactly controlling the size of nanocrystals is of great importance in the development of these materials, as this will lead to nano-objects with well-defined and reproducible properties. Whereas this goal seems to be hard to achieve with large nanocrystals, it might be viable for clusters consisting of a few tens or hundreds of atoms, as in this size regime a handful of structures can have an exceptionally high stability and therefore would form preferentially over any other combination of atoms. This concept is already well-known for several metal clusters, as for some of them several “magic” structures exist that are formed by closed shells of atoms.^[4–7] Cluster molecules that can be considered as the smallest building units of semiconductors have been investigated in the past.

As an example several tetrahedral cluster molecules based on the general formula $[E_wM_x(SR)_y]^{z-}$ (where E = S or Se; M = Zn or Cd; and R = alkyl or aryl) or similar were reported some years ago.^[8,9] The series was formed only by clusters

containing a well-defined number of atoms, and therefore, characterized by particularly stable structures; thus, these structures can also be termed “magic-size clusters” (MSCs). Different families of almost monodisperse CdS clusters of sizes down to 1.3 nm were reported by Vossmeier et al.,^[10] whereas CdSe MSCs were observed later in the solution growth of colloidal nanocrystals^[11] and the various cluster sizes found were explained as arising from the aggregation of smaller clusters. Soloviev et al. synthesized and crystallized a homologous series of CdSe cluster molecules^[12,13] (very similar in structure to those reported earlier^[8,9]) that were capped by selenophenol ligands. Also in many high-temperature organometallic syntheses of colloidal CdSe nanocrystals, either the transient formation of ultrasmall, highly stable CdSe clusters was noticed,^[14,15] or these clusters could be isolated using size-selective precipitation.^[16,17] Recently, one type of CdSe MSC has been synthesized in a water-in-oil reverse-micelle system.^[18]

Here, we report a method for controlling the sequential growth in solution of CdSe MSCs of progressively larger sizes. Each of these types of clusters is characterized by a sharp optical-absorption feature at a well-defined energy. During the synthesis, the relative populations of the different families of MSCs varied, as smaller MSCs evolved into larger MSCs. We can model the time evolution of the concentration of the various magic sizes using a modification of a continuous-growth model, by taking into account the much higher stability of the various MSCs over nanocrystals of any intermediate size.

For the synthesis of the CdSe MSCs reported here a mixture of dodecylamine and nonanoic acid was used to decompose cadmium oxide at 200 °C under an inert atmosphere. The resulting solution was stabilized at 80 °C and a stock solution of selenium in trioctylphosphine was injected into the flask. The temperature was kept at 80 °C throughout the synthesis. The low temperature ensured both slow nucleation and growth, as it produced large activation barriers for the two processes. The optical spectra of several aliquots taken during the synthesis are shown in Figure 1a. Some minutes after the injection, two well-defined absorption peaks appeared at 330 and 350–360 nm, as well as a shoulder around 384 nm. Over time, the peak at 330 nm disappeared, the peak at 360 nm kept losing intensity, the shoulder at 384 nm became a well-distinct peak, and a new peak showed up at 406 nm. Later, another shoulder appeared at longer wavelengths, which developed into a new absorption peak centered at 431 nm, followed by yet another peak at 447 nm. The position of all these peaks remained constant over time, whereas their rela-

[*] Dr. L. Manna, S. Kudera, A. Rizzo, Dr. Y. Li, Prof. G. Gigli, Prof. R. Cingolani, Dr. G. Ciccarella
National Nanotechnology Laboratory of CNR-INFN
Distretto Tecnologico – ISUI
Via Arnesano, 73100 Lecce (Italy)
E-mail: liberato.manna@unile.it

S. Kudera, M. Zanella, Prof. W. J. Parak
Center for Nanoscience
Ludwig Maximilians Universität
Amalienstraße 54, 80799 München (Germany)

Dr. C. Giannini
CNR-Istituto di Cristallografia (IC)
Via Amendola 122/O, 70126 Bari (Italy)

Dr. W. Spahl
Department of Chemistry and Biochemistry
Ludwig Maximilians Universität
Butenandtstr. 5-13 F, 81377 München (Germany)

[**] S. Kudera and M. Zanella contributed equally to this work. This work was supported by the European projects SA-NANO (contract number STRP 013698) and OLLA (contract number IST 004607), by the Italian MIUR 297 project (contract number 13587) by the Italian project FIRB NG-lab (contract number RBLA03ER38) and by the German research foundation (DFG, Emmy Noether program). We acknowledge Dr. Davide Cozzoli, Dr. Elvio Carlino, and Hermann Gumpff for many inspiring discussions. Supporting information is available online from Wiley InterScience or from the author.

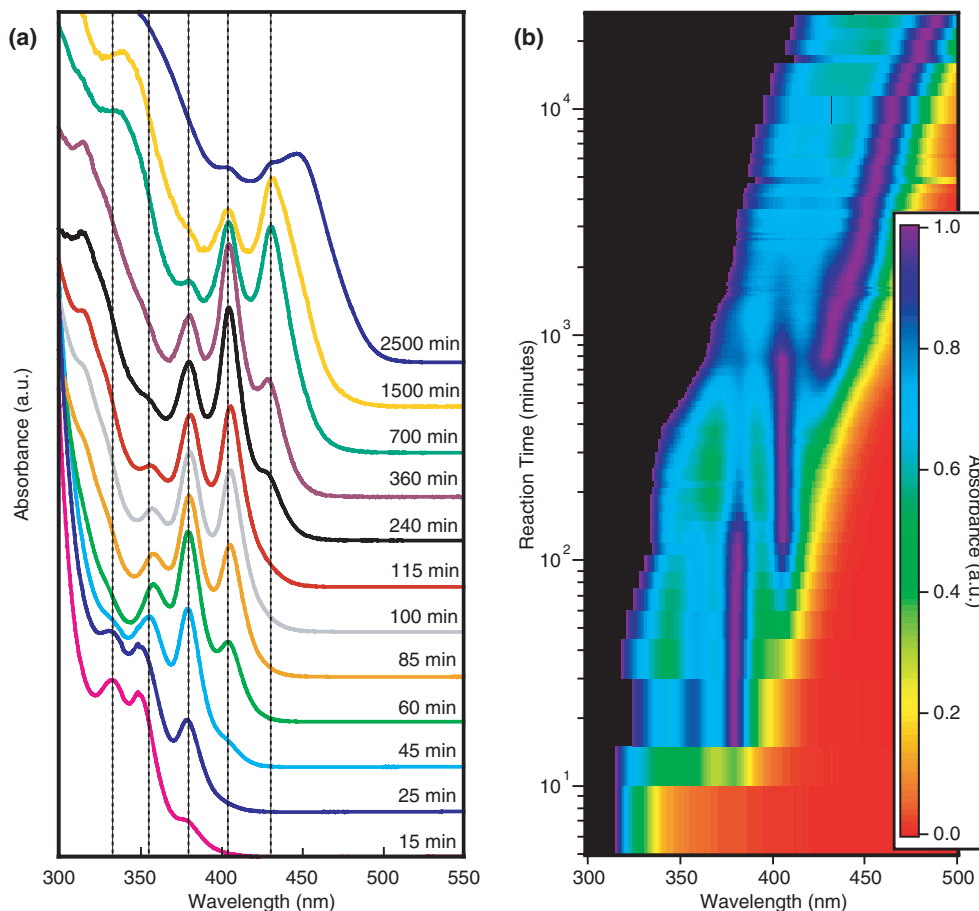


Figure 1. a) Absorption spectra of the growth solution recorded at different times and containing different populations of MSCs. b) This graph is built by stacking several horizontal stripes on top of each other, each of which corresponds to a color-coded plot of an optical-absorption spectrum, which were collected at progressively longer reaction times.

tive intensities varied so that the peak at the longest wavelength exhibited increasing intensity with respect to those at shorter wavelength, which eventually disappeared.

This behavior points to a size evolution through different families of increasingly larger clusters with high stabilities. If in fact these peaks corresponded to various excitonic transitions of a single family of cluster sizes in solution, and these clusters were steadily growing in size, then the spectral positions of the peaks would be shifting gradually towards longer wavelengths, and in addition their relative separation and their width would change (as their electronic structure is strongly sensitive to size^[19]). Instead, the time evolution of the optical spectra did not point to a continuous growth but rather to the formation of new families of MSCs having larger sizes. Also the optical emission spectra of diluted samples of the growth solution showed the contribution of different families of MSCs (see Supporting Information). Over time, the average cluster size within each family remained constant, whereas the relative population of the various families changed in favor of the one with the largest size.

The graph in Figure 1b is built by stacking several horizontal stripes on top of each other, each of which corresponds to

a color-coded plot of an optical absorption spectrum that had been collected at progressively longer reaction times. Each spectrum, that is, each horizontal stripe, is normalized to the intensity of its dominant peak. Spectra were recorded roughly every 15 min. On the overall plot, therefore, the wavelength is reported on the horizontal axis, whereas the reaction time is reported on the vertical axis. At shorter reaction times ($t < 10^2$ min) only a limited number of spectra could be collected and therefore the corresponding plots were replicated along the time scale until a new plot was available. As a consequence of this approach in constructing the overall plot, artificially sharp transitions are seen in it at these short times. The overall plot shows clearly the persistence over time of the peaks at 350–360 nm, 384 nm, 406 nm, and 431 nm, which therefore appear as vertical stripes. Once the various families of MSCs have evolved such that the peaks at 431–447 nm are the most intense ones, the overall spectral trends reflect rather the “continuous” size evolution of traditional nanocrystal growth kinetics.

The width of the various absorption peaks (see Fig. 1a) suggests that the size distribution within each family was quite narrow. As an example, the width-at-half-maximum of the

peak centered at 406 nm was approximately 20 nm (150 meV), which is rather close to the one reported by Kasuya et al.^[18] for ultrasmall, extremely monodisperse CdSe nanoparticles prepared in reverse micelles and absorbing strongly at 415 nm (also approximately 20 nm or only slightly narrower). The overall growth kinetics did not change much neither for syntheses carried out at lower temperatures (peak widths could not be narrowed further) nor at moderately higher temperatures (peak widths were slightly broader), as in both cases the changes over time in the relative populations of the various families of MSCs followed the same trend as above.

The mechanism by which the growth of these clusters proceeded in solution is definitely fascinating. At the very simplest level, the size evolution of a nanocrystal can be thought of as being the result of a competition between the attachment and detachment of single atoms to its surface. Based on this picture, we have developed a growth model that reproduces the time evolution of the relevant absorption features of the various families of MSCs. The experimental parameters for the various families of MSCs were extracted by performing a Gaussian deconvolution of the absorption spectra. For this fit we assumed that the contribution of a single family of MSCs consisted of a narrow Gaussian function that represents the lowest exciton peak and of a much broader Gaussian that models the absorbance at shorter wavelengths (see the Supporting Information for details). The key assumption of our model states that once a cluster has grown to a magic size, such a size is so stable that no atoms can detach from it. Therefore it can only grow further, but it cannot shrink. Any cluster with a size intermediate between two magic sizes can either grow to reach the larger of the two magic sizes, or shrink to the smaller one. Figure 2 reports with different marker types the intensities of the exciton peaks from the various families of MSCs over reaction time as derived from the fit to the experimental spectra, whereas solid lines represent the trends in the intensities of such peaks as derived from the pro-

posed growth model. This fitting procedure reflects qualitatively the actual trends in the growth of the various families of MSCs.

A control experiment that supports our model was carried out. A synthesis of MSCs was performed and thereby the nanocrystals were extracted from the solution using precipitation and purified by repeated washing. This sample, which contained different families of MSCs, was redissolved in the same mixture of surfactants used for the synthesis of MSCs and the mixture was heated at 80 °C for several hours. Therefore, all conditions were similar to those used for the synthesis of MSCs, with the only difference being that no free monomers were present in this experiment. Optical-absorption spectra on aliquots taken from this mixture at different times during the heating did not show any remarkable variation in the intensity of the various peaks, nor any shift in their positions, indicating no further evolution in the distribution of the families of MSCs. The results of this control experiment have two important implications. One is that the various MSCs were stable and that they did not undergo any shrinking or ripening process, as opposed to the classical case of a sample containing a wide distribution of colloidal crystal sizes, for which Oswald-ripening processes dominate if there is a shortage of monomers.^[20] The other is that no aggregation occurred among smaller clusters to form larger clusters. Both implications support our growth model.

The novelty of the synthetic approach developed here is that it yields only MSCs. These are not a side product of a synthesis that yields much larger nanocrystals, nor are much larger nanocrystals formed as a side product in our syntheses. Furthermore, as the growth is slow, the synthesis is reproducible and indeed it can be stopped whenever a given distribution of various families of MSCs is reached. Then, from this final solution, the largest family of MSCs present can be isolated using a size-selective precipitation. A typical set of optical absorption spectra before and after size-selective precipitation is reported in Figure 3a. The isolation of MSCs of smaller sizes from this solution is in principle possible but laborious, as they are contaminated by a small percentage of the largest MSCs.

Transmission electron microscopy (TEM) analysis on aliquots extracted from the growth solution and on size-selected samples revealed that these MSCs have roughly spherical shapes and that they are not aggregated. However, a more detailed analysis based on electron microscopy and aimed at determining average sizes and size distributions was strongly limited by the extremely small sizes of such clusters. Wide-angle X-ray diffraction analysis on size-selected samples indicated cluster sizes ranging from 1.5 to 2.0 nm for the families of largest MSCs (those absorbing strongly at 406, 431, and 447 nm, respectively) and elemental analysis of these size-selected and purified clusters showed that they are all Cd-rich, with Cd/Se ratios ranging from 1.1 to 1.3. No further structural information could be inferred from mass spectrometry, as the ionization of these samples in a matrix-assisted laser desorption ionization time-of-flight mass spectrometry (MALDI-

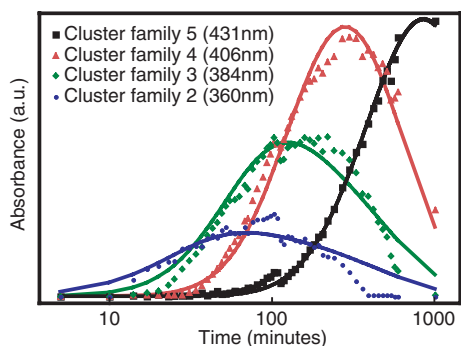


Figure 2. Development over time of the intensities of the individual absorption peaks from the various MSCs. These were extracted from the normalized optical absorption spectra, as shown in Figure 1. The families of smallest MSCs as identified from the optical spectra (those showing a peak at 330 nm) were not considered in the fit, as their absorption spectra became too weak a few minutes after their formation. Solid lines represent the fits to these trends using the proposed growth model.

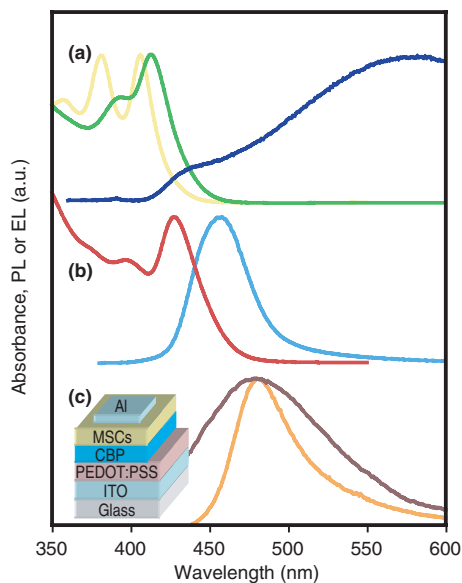


Figure 3. a) Optical absorption spectra of a sample (yellow) before size-selective precipitation, and optical absorption (green) and fluorescence spectra (blue) after size-selective precipitation. b) Optical absorption (red) and fluorescence spectra (cyan) of the CdSe/ZnS core/shell nanocrystals prepared from the size-selected sample of MSCs shown in (a). c) Photoluminescence from a film of core/shell nanocrystals (light brown) and EL (brown) from a light-emitting diode based on these nanocrystals. The inset displays the schematic layout of the EL device.

TOF-MS) setup yielded very similar fragmentation patterns, even for nanocrystals as large as 3 nm in diameter, but did not yield any clear fingerprints of the original clusters.

The synthesis of different families of MSCs is of technological interest as it yields nanocrystals that always have the same sizes and, therefore, reproducible optical properties, such as, for instance, the range of emitted light. The CdSe clusters reported in this work displayed considerable emission from trap states (see Fig. 3a) and band-edge emission was only clearly visible at very high dilutions. So, after size-selective precipitation, the absorption features were slightly broadened and red-shifted. Both effects could be the result of stripping off of some molecules from the surface of the MSCs during cleaning. This might have resulted in a partial reconstruction of the nanocrystal surface, with a concomitant variation of the overall electronic properties of the clusters.^[21,22] By adding fresh surfactants, we could partially cancel this effect. Light emission from these clusters occurred almost exclusively from trap states. However, when a ZnS shell was grown on the size-selected nanocrystals, such as, for instance, on those originally absorbing at 406 nm, the resulting core/shell nanocrystals emitted only from band-edge states (Fig. 3b). The photoluminescence (PL) quantum yield from these samples varied from synthesis to synthesis (in the range between 35 and 60%), but remained constant for each sample, even for a few months after the synthesis.

A potential application of the blue-light-emitting nanocrystals synthesized in this work is, for instance, a light-emitting

diode. There have been several studies of nanocrystal-based light-emitting diodes in the last years,^[23–28] but only a few devices have been reported so far in which the blue emission originated from nanocrystals.^[26] We built a blue-light-emitting diode in which the active layer was a blend of the blue-light-emitting CdSe/ZnS nanocrystals, prepared as described above, and 4,4',N,N'-diphenylcarbazole (CBP). The device, whose geometry and characteristics are displayed in Figure 3c, showed an electroluminescence (EL) peak at 485 nm, which is attributed to the emission of the CdSe/ZnS nanocrystals, in agreement with the PL spectra from a solid film of the same nanocrystals (Fig. 3c). The red-shift in the emission for the clusters in the film relative to that for the clusters in solution is attributed to the energy transfer within the sample.^[29] The increase in peak width of the EL is likely to be an effect of both environmental broadening and local heating of the sample under current flow.^[25]

In conclusion, we have reported a method to control the sequential growth of CdSe magic-size clusters of progressively larger sizes. We modeled the time evolution of the concentration of the various magic sizes using a slight modification of a continuous-growth model. After the synthesis, we could isolate MSCs of a given size and grow a ZnS shell on them. Finally, we demonstrated the fabrication of a hybrid organic/inorganic light-emitting diode based on these nanocrystals with blue-light emission. The concept of sequential growth of different families of MSCs reported here is of general interest and can be potentially extended to other materials, provided that suitable conditions are found to slow down the nucleation and the growth rate of the nanocrystals. In addition, we believe that this approach can be followed to synthesize more elaborate nanostructures, such as, for instance, doped nanocrystals.^[30–36] A route to prepare doped nanocrystals could for instance be through the controlled formation of extremely small clusters, such as those reported in this work, but having a certain number of doping atoms already embedded in them. It might be likely, for instance, that such small cluster molecules could gain an additional stability (and therefore could be formed preferentially) if one or more “impurity atoms” were present in their structure. This possibility is currently under investigation in our groups.

Experimental

Synthesis of Magic-Size CdSe Nanocrystals: 1 g of cadmium oxide (99.99%), 4 g of dodecylamine (98%), and 4 g of nonanoic acid (97%) were mixed in a three-necked flask. The flask was pumped to vacuum at 100 °C for 15 min and then heated to above 200 °C under nitrogen to decompose the CdO. The temperature was then lowered to 80 °C and 20 g of a solution of Se in trioctylphosphine (10% in weight of Se) was injected. After the injection the temperature dropped and it was allowed to recover to 80 °C (but not higher). During the growth, 0.1 mL of the growth solution was extracted at time intervals ranging from 3 min (at the early stages of growth) to several hours (after several hundred minutes of growth) and diluted into a known amount of toluene. Therefore, all spectra could be scaled according to the dilution factor.

Size-Selective Precipitation: After the synthesis, the growth solution was transferred to a glove-box. Ethyl acetate was added to this solution, followed by methanol until a persistent cloudiness was observed. An amount of methanol ranging from 50 to 150 mL was required, depending on the distribution of MSCs present in the solution. Ethyl acetate was needed to prevent phase segregation, as methanol and trioctylphosphine have a low miscibility. This solution was centrifuged and the precipitate was washed again by adding few milliliters of ethyl acetate and methanol. The final precipitate was redissolved in toluene. By using this procedure, the largest MSCs are almost quantitatively separated from the smaller MSCs present.

ZnS Shell Growth: This was carried out following standard published procedures [37], except for the shell-growth temperature, which was set at 80 °C for the first injection and then steadily raised to 120 °C during the following injections. The starting MSCs could not resist the heating in trioctylphosphine/trioctylphosphine oxide above 80 °C for too long.

Fabrication and Characterization of the Electroluminescent Devices: Devices consisting of ITO/PEDOT-PSS/CBP:CdSe/ZnS/Al were fabricated as follows. A hole-transporting layer (100 nm) of poly(3,4-ethylenedioxythiophene):poly(styrenesulfonate) (PEDOT:PSS), used to lower the hole-injection barrier at the indium tin oxide (ITO) surface, was spin-deposited onto a cleaned ITO-coated glass substrate (120 nm, $15 \Omega \text{square}^{-1}$). The layer was then heated at 110 °C for 10 min to remove residual solvent. Then, a layer of a blend of CdSe/ZnS nanocrystals and CBP (100 nm) was spin-coated from a chloroform solution on the surface of the PEDOT:PSS layer. Finally, a 150 nm thick Al layer was deposited by thermal-evaporation at a pressure of 4×10^{-6} mbar (1 bar = 10^5 Pa). PL spectra were recorded on thin films and CHCl_3 solutions, by using a Cary Eclipse fluorescence spectrophotometer with an intense Xenon flash lamp. Absorption measurements were carried out using a Cary 5000 UV-vis spectrophotometer. The EL spectra were measured by a Spectroradiometer OL 770. All the measurements were carried out at room temperature under air.

Received: May 9, 2006

Revised: September 18, 2006

Published online: January 24, 2007

- [1] X. Michalet, F. F. Pinaud, L. A. Bentolila, J. M. Tsay, S. Doose, J. J. Li, G. Sundaresan, A. M. Wu, S. S. Gambhir, S. Weiss, *Science* **2005**, *307*, 538.
- [2] I. L. Medintz, H. T. Uyeda, E. R. Goldman, H. Mattoussi, *Nature Mater.* **2005**, *4*, 435.
- [3] W. J. Parak, T. Pellegrino, C. Plank, *Nanotechnology* **2005**, *16*, R9.
- [4] J. Pedersen, S. Bjornholm, J. Borggreen, K. Hansen, T. P. Martin, H. D. Rasmussen, *Nature* **1991**, *353*, 733.
- [5] T. P. Martin, T. Bergmann, H. Gohlich, T. Lange, *J. Phys. Chem.* **1991**, *95*, 6421.
- [6] T. P. Martin, *Phys. Rep.* **1996**, *273*, 199.
- [7] W. Ekardt, *Z. Phys. B: Condens. Matter* **1997**, *103*, 305.
- [8] G. S. H. Lee, D. C. Craig, I. Ma, M. L. Scudder, T. D. Bailey, I. G. Dance, *J. Am. Chem. Soc.* **1988**, *110*, 4863.
- [9] N. Herron, J. C. Calabrese, W. E. Farneth, Y. Wang, *Science* **1993**, *259*, 1426.
- [10] T. Vossmeier, L. Katsikas, M. Giersig, I. G. Popovic, K. Diesner, A. Chemseddine, A. Eychmüller, H. Weller, *J. Phys. Chem.* **1994**, *98*, 7665.
- [11] V. Platschek, T. Schmidt, M. Lerch, G. Müller, L. Spanhel, A. Emmerling, J. Fricke, A. H. Foitzik, E. Langer, *Ber. Bunsenges. Phys. Chem.* **1998**, *102*, 85.
- [12] V. N. Soloviev, A. Eichhöfer, D. Fenske, U. Banin, *J. Am. Chem. Soc.* **2000**, *122*, 2673.
- [13] V. N. Soloviev, A. Eichhöfer, D. Fenske, U. Banin, *J. Am. Chem. Soc.* **2001**, *123*, 2354.
- [14] H. Z. Wang, A. Tashiro, H. Nakamura, M. Uehara, M. Miyazaki, T. Watari, H. Maeda, *J. Mater. Res.* **2004**, *19*, 3157.
- [15] Z. A. Peng, X. G. Peng, *J. Am. Chem. Soc.* **2002**, *124*, 3343.
- [16] C. B. Murray, D. J. Norris, M. G. Bawendi, *J. Am. Chem. Soc.* **1993**, *115*, 8706.
- [17] A. L. Rogach, A. Kornowski, M. Y. Gao, A. Eychmüller, H. Weller, *J. Phys. Chem. B* **1999**, *103*, 3065.
- [18] A. Kasuya, R. Sivamohan, Y. A. Barnakov, I. M. Dmitruk, T. Nirasawa, V. R. Romanyuk, V. Kumar, S. V. Mamykin, K. Tohji, B. Jayadevan, K. Shinoda, T. Kudo, O. Terasaki, Z. Liu, R. V. Belosludov, V. Sundararajan, Y. Kawazoe, *Nat. Mater.* **2004**, *3*, 99.
- [19] A. L. Efros, M. Rosen, *Annu. Rev. Mater. Sci.* **2000**, *30*, 475.
- [20] T. Sugimoto, *Adv. Colloid Interface Sci.* **1987**, *28*, 65.
- [21] A. Puzder, A. J. Williamson, F. Gygi, G. Galli, *Phys. Rev. Lett.* **2004**, *92*, 217401.
- [22] J. Frenzel, J. O. Joswig, P. Sarkar, G. Seifert, M. Springborg, *Eur. J. Inorg. Chem.* **2005**, 3585.
- [23] S. Coe, W. K. Woo, M. Bawendi, V. Bulovic, *Nature* **2002**, *420*, 800.
- [24] N. Tessler, V. Medvedev, M. Kazes, S. H. Kan, U. Banin, *Science* **2002**, *295*, 1506.
- [25] J. L. Zhao, J. Y. Zhang, C. Y. Jiang, J. Bohnenberger, T. Basche, A. Mews, *J. Appl. Phys.* **2004**, *96*, 3206.
- [26] J. S. Steckel, J. P. Zimmer, S. Coe-Sullivan, N. E. Stott, V. Bulovic, M. G. Bawendi, *Angew. Chem. Int. Ed.* **2004**, *43*, 2154.
- [27] Y. Q. Li, A. Rizzo, M. Mazzeo, L. Carbone, L. Manna, R. Cingolani, G. Gigli, *J. Appl. Phys.* **2005**, *97*, 113501.
- [28] S. Coe-Sullivan, J. S. Steckel, W. K. Woo, M. G. Bawendi, V. Bulovic, *Adv. Funct. Mater.* **2005**, *15*, 1117.
- [29] C. R. Kagan, C. B. Murray, M. G. Bawendi, *Phys. Rev. B: Condens. Matter* **1996**, *54*, 8633.
- [30] F. V. Mikulec, M. Kuno, M. Bennati, A. D. Hall, R. G. Griffin, M. G. Bawendi, *J. Am. Chem. Soc.* **2000**, *122*, 2532.
- [31] D. J. Norris, N. Yao, F. T. Charnock, T. A. Kennedy, *Nano Lett.* **2001**, *1*, 3.
- [32] K. M. Hanif, R. W. Meulenberg, G. F. Strouse, *J. Am. Chem. Soc.* **2002**, *124*, 11495.
- [33] D. Yu, C. J. Wang, P. Guyot-Sionnest, *Science* **2003**, *300*, 1277.
- [34] D. A. Schwartz, N. S. Norberg, Q. P. Nguyen, J. M. Parker, D. R. Gamelin, *J. Am. Chem. Soc.* **2003**, *125*, 13205.
- [35] S. C. Erwin, L. J. Zu, M. I. Haftel, A. L. Efros, T. A. Kennedy, D. J. Norris, *Nature* **2005**, *436*, 91.
- [36] N. Pradhan, D. Goorskey, J. Thessing, X. G. Peng, *J. Am. Chem. Soc.* **2005**, *127*, 17586.
- [37] B. O. Dabbousi, J. Rodriguez Viejo, F. V. Mikulec, J. R. Heine, H. Mattoussi, R. Ober, K. F. Jensen, M. G. Bawendi, *J. Phys. Chem. B* **1997**, *101*, 9463.